Lithuanian Journal of Physics, Vol. **50**, No. 4, pp. 451–462 (2010) doi:10.3952/lithjphys.50404

ESTIMATION OF THE PERMANENT DIPOLE MOMENT OF BACTERIORHODOPSIN

B.P. Kietis [a], M. Macernis [b], J. Sulskus [b], and L. Valkunas [a,b]

[a] *Center for Physical Sciences and Technology, Institute of Physics, Savanorių 231, LT-02300 Vilnius, Lithuania*
E-mail: mindaugas.macernis@ff.vu.lt

[b] *Department of Theoretical Physics, Faculty of Physics, Vilnius University, Saulėtekio 9, LT-10222 Vilnius, Lithuania*

Received 16 November 2010; revised 1 December 2010; accepted 15 December 2010

The static electric dipole moment persisting in bacteriorhodopsin was defined from electro-acoustic measurements of the dried films of purple membranes and compared with the value estimated from quantum chemical calculations. The projection of this value normal to the membrane surface is experimentally estimated to be equal to 40 D and oriented from the cytoplasmic side to the extracellular side of the membrane. This value is almost independent of the environment pH. QM/MM calculations were also performed for the known structures of the ground and intermediate states of bacteriorhodopsin. According to calculations the dipole moment is mainly determined by the cytoplasmic and extracellular coils, while the contribution from the transmembrane helices is smaller and of the opposite direction, and this value corresponding to the active centre is small. The calculated values of the dipole moment of bacteriorhodopsin in the intermediate states K, L, and M provide understanding about the origin of the driving force for the proton pumping. Employing the values of the dipole moments corresponding to the ground and intermediate states of bacteriorhodopsin, defined by means of QM/MM calculations, the experimentally determined photoelectric response of the dried films is explained.

Keywords: dried films of purple membranes, electrostriction, photo-electric response, pH changes, molecular mechanics calculations, quantum chemical calculations

PACS: 87.14.ep, 77.65.-j, 82.80.Yc, 83.10.Rs, 03.65.-w

1. Introduction

Bacteriorhodopsin (BR) is the membrane protein implementing the active proton pumping through the purple membrane (PM) of *Halobacterium salinarum* [1] after the green light absorption by retinal. The protein arranged as a bundle of seven transmembrane helices, and the retinal chromophore bound to the Lys 216 residue via a protonated Schiff base are the main two constituents of the BR monomer [2]. Site directed mutagenesis combined with various spectroscopic methods, crystallographic studies, and molecular dynamic simulations revealed many details of the structure and its changes in the course of the BR photocycle [3]. However, a number of questions concerning electrodynamics and electrostatics of this photoactive protein, which is believed to be of a particular technological interest, is still unanswered.

Membrane proteins are asymmetric in most cases due to the presence of surface electric charges and dipoles [4–9]. Possibilities of orientation of the PM evidently confirm the existence of a permanent dipole moment at low frequencies and an induced dipole moment at high frequencies of the applied field [10–14]. This electric asymmetry seems to be responsible for the proton driving through the membrane [15].

Possible role of the permanent dipole moment in support of the proton transfer in BR as a result of attraction of protons into the cell and repulsion of protons out of the cell has been already suggested [16]. So far the assignment of the dipole moment (DM) has been deduced from the electro-optical measurements performed at different frequencies. However, the result can be conditioned by a large number of different factors. Indeed, the value of the DM of the PM is strongly dependent on the size of the membrane disc, the concentration of the PM fragments, and polarity of the environment perturbing the membrane surface [12, 16–18]. Hence, the conclusion about the nature of electric parameters of the PM is not a trivial task.

Most of experiments, which could define the charge asymmetry, indicate a negative charge on the cytoplasmic side, unless pH of the environment is low [20, 21]. It has been demonstrated that the orientation of the membrane discs and the migration of the membrane

ISSN 1648-8504

fragments in an electrophoretic flow can be essentially affected by a quasi-static electric field [6]. From the sign of the photoresponse signal it has been deduced that the cytoplasmic side is charged more negatively when pH is higher than 5 and vice versa when pH is less than 5 [22], while at pH 5 both sides are almost equally charged [22, 23]. However, in accord with predictions [12] the inverse DM of the BR molecule under the normal external conditions directed from the cytoplasmic side to the extracellular side has been identified from studies of the dried PM films [15]. Hence the dehydratation of the sample should have a crucial impact on the electric asymmetry of the PM. The internal DM of the PM in dried films causes their electrostrictive properties, which could be invoked for direct estimations of the value of the internal field [15]. As will be shown bellow, this value remains unchanged in the dried PM film even when pH is low, thus supporting the assumption of a different origin of this dipole moment than that detected in aqueous suspensions.

To understand a possible reason of such variability of the DM in BR depending on the exterinal conditions (solutions versus dried films) and to identify the origin of this value defined from the electro-acoustic and light-induced electric measurements is the main task of our studies. Evidently, this relationship might be affected by various external contributions. For instance, by changing pH of the solution we should apparently change the electric conductivity of the sample and thus affect on the photoelectric response of the sample. For quantum chemical calculations of the DM we use the crystallographic data of BR. This structure better correlates with the PM in the dried films and not in solutions. Moreover, the photoelectric response is usually defined from relevant measurements of the dried films [15, 24], thus, the calculated DM should be compared with the value deduced from the experimental measurements of the dried films.

2. Methods

2.1. Experimental studies

2.1.1. Electro-acoustic measurements

The static electric dipole moment persisting in the dried PM film can be defined by analysing electrostrictive properties of the film (see [15] for the experimental details). The electrostriction is defined by the following relationship:

$$S = \frac{\xi}{2c} E^2 \,, \tag{1}$$

where E is the electric field acting on the system under consideration, S is the mechanical deformation induced by the field, and c is the elasticity of the material. According to definitions [25] the electrostriction coefficient $\xi = \varepsilon_0 \rho \mathrm{d}\varepsilon/\mathrm{d}\rho$, where ε_0 is the vacuum permittivity, ρ is the density of the material, and ε is the permittivity of the sample. The electric field acting on the material is composed of the internal electric field E_P due to the presence of the dipoles and of the external electric field E_ex, thus giving $E = E_\mathrm{P} + E_\mathrm{ex}$. The main idea of this method is to subject the PM film to a combined external field $E_\mathrm{ex} = E_\mathrm{0ex} + E_{\sim\mathrm{ex}}$, where E_0ex is the static component and $E_{\sim\mathrm{x}}$ is the alternating component of the electric field. Hence, in this case $E = E_\mathrm{P} + E_\mathrm{0ex} + E_{\sim\mathrm{ex}}$. Substituting this value into Eq. (1) and assuming that $E_\mathrm{0ex} \gg E_{\sim\mathrm{ex}}$, the variable component of the deformation $S_\sim$ could be expressed as

$$S_\sim = \frac{\xi}{c} \left(E_\mathrm{P} + E_\mathrm{0ex}\right) E_{\sim\mathrm{ex}} \,. \tag{2}$$

According to this expression it is possible to define the internal electric field E_P, which is inherent in the dried PM film as well as in dried films of any type.

The direction and strength of external field E_0ex can be easily adjusted to compensate for the internal electric field E_P persisting in the film, thus, giving $E_\mathrm{P} + E_\mathrm{0ex} = 0$, which for a particular thickness of the film satisfies the same equality for voltages

$$U_\mathrm{P} = -U_\mathrm{C\,0ex} \,, \tag{3}$$

where U_P is the polarization potential and $U_\mathrm{C\,0ex}$ is the critical value of external voltage U_0ex corresponding to $S_\sim = 0$. If this condition for the external voltage $U_\mathrm{C\,0ex}$ is fulfilled, the alternating deformation of the film is reduced to zero, $S_\sim = 0$. The latter is the required condition in determining the value of polarization potential U_P of the material under investigation. Thus, this value has the meaning of the critical potential of electrostriction. Under experimental conditions of the closed electric circuit, the extracted heat as a result of the electric current causes restrictions for applicability of this approach. Therefore, this method cannot be applied under humid conditions, when changes of pH values due to the electrolysis are expected.

2.1.2. Preparation of dried films

Suspension of the purple membranes was obtained from *Halobacterium salinarum* strain S9 by means of a standard procedure [1]. The dried PM films used for comparative studies of the electro-acoustic measurements have been prepared from the suspension by

the electrophoretic deposition of the PMs on a ITO (indium-tin-oxide) conducting glass connected as the anode in the electric circuit [26]. The surface area of the film was about 0.5 cm^2 in size. The ITO layer is a light-transparent electrode typically used for measurements of the photoelectric potential of the film. The photoelectric response of the samples and kinetics corresponding to the L and M intermediates qualitatively coincides with kinetics corresponding to BR [22].

For acidification of the films a known technological procedure [24] was invoked. The pH value of the dried film cannot be defined precisely, however, the impact of the pH is visually distinguished from colour changes of the film. Further on we will use notation "low pH" for the dried PM film, which was treated with HCl solution (pH2) for 3 minutes and then dried in the air. The pH effects were completely reversible and the PMs were not degraded by the pH treatment.

2.1.3. Photo-induced electric response (PERS)

Second harmonic (532 nm) of the Q-switched Nd:YAG laser was used for the optical excitation of the sample. The energy of the excitation light pulse was ≈10 mJ, pulse duration ≈3 ns. The voltage generated by light depends on the orientation of the film and can reach up to 2 volts for the well-oriented film. The PERS experimental results were obtained by averaging 50 separate photoresponses. The resistance of the dried films was of the order of 10^{11} Ω, while the humidity of the environment during the experiments was about 60% at 20 °C. The experimentally measured capacitance of the film was equal to $C_{\text{film}} = 3.2{\cdot}10^{-10}$ F. For PERS measurements the load resistance was chosen to be 10^{10} Ω and the capacitance was of the order of 10^{-11} F [27].

2.2. Theoretical approach

Numerical estimations of the charge distribution reflect the structural complexity of the molecule under investigation. For DM calculations, known structures of BR in the initial and subsequent K, L, and M states are analysed in terms of the QM/MM method. The obtained DM values are projected on the z axis pointed from the cytoplasmic side to the extracellular side. The structural data are taken from the PDB bank. A subsequent structural data optimization via energy minimization was invoked [28]. For this purpose we use the structures corresponding to the ground state and to the intermediates K, L1, M1. The 1C3W structure from the PDB bank [29] is attributed to the ground (BR1) structure, while the 1M0K structure [30] is taken as corresponding to the K state (BR-K). The 2NTW structure [31] is chosen for calculations of the protein configuration in the L1 state. Similarly, the 1M0M structure [32] is taken for calculations in the M1 state (BR-M1).

Several packages are used for DM calculations and for the analysis of the results. The DM calculations are performed using the Amber 9 MD package [28]. The BR structure is qualified by taking the *leaprc.ff03* force field into account [28]. For this purpose structures taken from the PDB bank are corrected according to the result observed by Swiss-PdbViewer [33]. QM calculations are performed with the Gaussian 03 quantum chemistry package [34] within the frame of the density functional theory, DFT [35] using B3LYP [36] functional and 6-31G* basis set. The topology files and charges in the system are generated by the *t-leap* program from the Amber package. The figures are drawn and the DM is calculated and analysed with VMD 1.8.7 [37], and the final data are analysed using MATLAB 7.5.

Additional hydrogen atoms are added during the calculations to the structures taken from the PDB bank, where it is needed. Since the Amber package [28] does not contain parameters relevant to the Schiff base connecting retinal to Lys 216 (the RETLYS structure) and for protonated ASP85, the appropriate parametrization was performed by invoking the Gaussian 03 quantum chemistry package [34] in the frame of DFT [35] using B3LYP functional [36] and the 6-31G* basis set. This approach is known as giving good results for the whole protein [28]. All other possible states were generated by the *t-leap* program from the Amber package.

3. Results

3.1. Experimentally determined permanent DM

Variable component of the deformation of the dried oriented PM film defined by means of electro-acoustic measurements at two different pH values is presented in Fig. 1. The orientation degree of the PMs in a particular film is a determining factor of the value of the photoelectric response as well as the zero point of the transformation function depending on the external DC voltage in the electro-acoustic measurements [15]. Hence, the same oriented PM film was used in all experiments presented in this paper. For comparative purposes the control experiments were also carried out with different PM films of various degrees of orientation (not shown).

According to rough estimations the pH value for the acid treated film should be of the order of 2. The critical

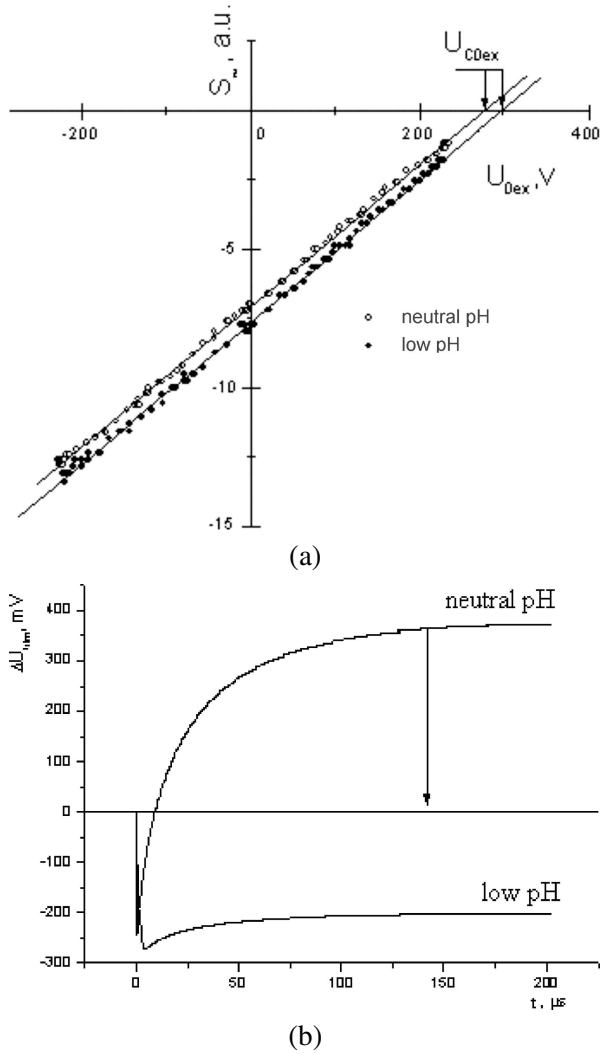

Fig. 1. (a) Variable component of the deformation of the dried oriented PM film defined by means of electro-acoustic measurements at two different pH values as indicated in figure and (b) the PERS of the same film at the same two pH levels. $U_{C\,0ex}$ is the critical value of external static voltage U_{0ex}, which compensates the internal electric persistent in the films, thus resulting in $S_\sim = 0$.

values of the bias voltage $U_{C\,0ex}$, defined as the crossing point with the abscissa axis, are 279 and 299 V for the normal and acid treated films, correspondingly. The positive potential (when ITO is held negative) is needed to compensate for the internal electric field of an opposite direction inherent in the PM film (Eq. 3). Hence, the internal DM of the BR molecule is directed from the cytoplasmic side towards the extracellular side of the membrane. The internal electric DM detected by the electroacoustic technique qualitatively is not dependent on pH variation (Fig. 1), which strongly contradicts the experimental observations carried out on the PM suspensions where the value of the permanent DM of BR varies up to changing its direction depending on pH [12, 16–19].

Results presented in Fig. 1(a) allow us to directly determine the $U_{C\,0ex}$ values and to consequently estimate the value and direction of the DM corresponding to a single BR in the dried PM film. Our findings indicate the retinal–protein interaction to be directly connected to the electric polarization E_P corresponding to the dried oriented films of BR.

The electric potential difference U_P created by a dipole in one-dimensional system is

$$U_P = \frac{p_{BR}\,(2\alpha - 1)\,n_{BR}\,d}{\varepsilon\,\varepsilon_0}\,, \tag{4}$$

where p_{BR} is the DM projection to the axis normal to the membrane surface, n_{BR} is the concentration of dipoles, and d is the thickness of the film. Factor $2\alpha - 1$ reflects the orientation degree of PMs in the film [27]. Evidently, in disoriented film this factor equals zero and for totally oriented film it equals 1 since $\alpha = 0.5$ and $\alpha = 1$, respectively. By combining Eqs. (3) and (4) the DM of a single BR molecule can be estimated from the experimentally determined $U_{C\,0ex}$ value.

The concentration of the BR molecules can be determined as $n_{BR} = (V_{BR})^{-1}$, where V_{BR} is the volume corresponding to the BR molecule. Estimate of this volume gives $V_{BR} = 3.5{\times}4.5{\times}5{\cdot}10^{-27}$ m^3. The thickness d of the film, the vacuum permittivity ε_0, the relative dielectric constant $\varepsilon \approx 3$ [38], and the surface area of the electrode A can be related to the electric capacitance of the film: $C_{folm} = \varepsilon\,\varepsilon_0\,A/d$. The orientation factor of this film is known to be $\alpha \cong 0.65$ [27]. Thus, invoking the relationship $U_P \to -U_{C\,0ex}$ as follows from Eq. (3), the DM for a single BR, p_{BR} can be defined as

$$p_{BR} = -\frac{V_{BR}\,C_{film}\,U_{C\,0ex}}{(2\alpha - 1)\,A}\,. \tag{5}$$

The experimentally measured capacitance of the film reaches value $C_{film} = 3.2{\cdot}10^{-11}$ F, the surface area of the electrode equals to $A = 2{\cdot}10^{-5}$ m^2, and $U_{C\,0ex} \approx$ 300 V. Taking these values into account, the DM projection of the single BR molecule corresponds to the following estimation: $p_{BR} \approx 1.3{\cdot}10^{-28}$ C m or $p_{BR} \approx$ 40 D (1 D $\approx 3.3cdot10^{-30}$ C m). Evidently, such a big dipole moment cannot be attributed to the retinal chromophore only.

It is noteworthy that $U_{C\,0ex} \approx 300$ V is almost the same for the films under normal and low pH conditions (Fig. 1), which is in contrast to the results obtained in solutions [22]. This difference is due to reduction of the dissociation possibility under the dry conditions.

The PERS shown in Fig. 1(b) is sensitive to the acidification conditions of the dried film. Under normal con-

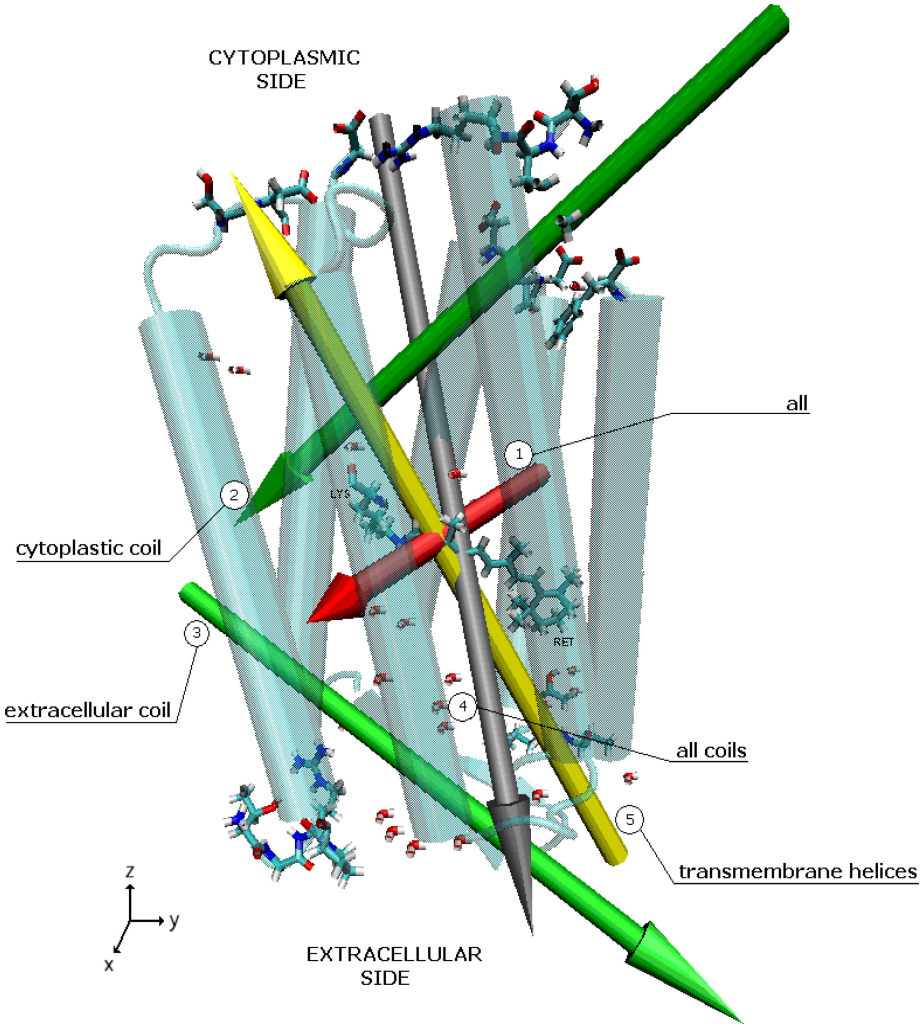

Fig. 2. The DM values defined for the 1C3W [29] structure. Arrows indicate the DM values corresponding to BR (*1*), cytoplasmic coil (*2*), extracellular coil (*3*), extracellular coil (*4*), all coils (*5*).

ditions the PERS of the film contains all phases appropriate for the active BR. The initial phase is negative and reflects the transformation from L to M states, while the kinetics corresponding to the latter is of the positive sign. The low pH film (acidic conditions) contains then an initial negative signal only indicating the presence of the L state, which, however, does not evolve to the M state anymore. This effect is related to the blockage of the proton transfer pathway to the first proton acceptor D85 by other proton from the external environment [27].

3.2. DM calculations

Calculations performed using the Amber 9 MD package [28] allow us to determine the DM for the BR1 structure taken from the crystallographic data [29] and also subsequently using the MM minimization of the structure. The monomer corresponding to BR1 consists of 2073 atoms (the hydrogen atoms not taken into account). Therefore, additional hydrogen atoms are added to the structures taken from the PDB bank, where it is needed. The protonated Schiff base as a constituent of the RETLYS residue is assumed to contain a positive charge in the course of the parametrization procedure. The obtained results of calculations are presented in Table 1. Interestingly, the total DM does not change too much by applying additional MM minimization. Its value for the crystallographic structure is equal to 257.02 D (the orientation of the DM is indicated by arrow *1* in Fig. 2), while the corresponding p_{BR} (projection of the value on the z axis) is -93.01 D. After MM minimization of the structure the DM slightly changes reaching 251.57 D in value with p_{BR} giving -71.74 D (see BR values in Fig. 3(a)). The positive direction of DM projection is assumed the direction from extracellular to cytoplasmic side (the positive direction of z axis in Fig. 2).

Table 1. The dipole moment (DM) and its projection value (p_{BR}) corresponding to the initial, K, L, and M intermediates of BR.

No	Structure	Type (PDB code)	p_{BR}	The DM value, D					
				BR	Protein	Trans-membrane helices	Cytoplasmic coil	Extracellular coil	All coils
1	BR1	X-ray (1C3W)	−93.01	257.02	401.68	574.98	502.41	554.45	614.34
2	BR1	minimized	−71.74	251.57	397.96	577.96	503.75	553.12	600.98
3	BR-K	X-ray (1M0K)	−83.43	248.87	387.80	609.45	361.14	559.98	651.23
4	BR-K	minimized	−57.86	226.82	385.61	619.77	343.03	557.51	600.51
5	BR-L1	X-ray (2NTW)	−114.26	254.40	398.87	576.02	516.97	558.41	639.94
6	BR-L1	minimized	−91.61	239.47	399.78	600.68	512.77	556.77	608.32
7	BR-M1	X-ray (1M0M)	−99.11	252.73	262.44	541.74	675.09	557.76	606.13
8	BR-M1	minimized	−41.95	232.55	247.46	566.38	667.33	555.58	580.81

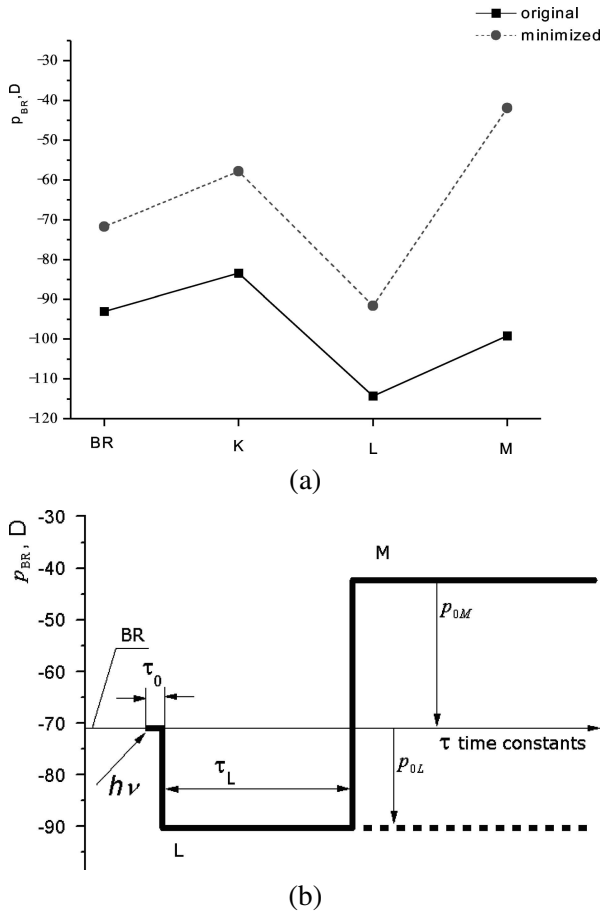

Fig. 3. (a) Projection of the DM on the z axis of the membrane defined by QM/MM calculations and (b) the time evolution of these values in a separate BR molecule. DM values calculated for BR [29], K [30], L [31], and M [3] intermediates.

For better understanding the main contributions by determining the DM value, calculations were also performed separately for the internal coil consisting of retinal and bound water molecules, for the cytoplasmic and extracellular coils, as well as for the transmembrane helices. The calculated DM value for the cytoplasmic coil is equal to 502.41 D as indicated by arrow *2* in Fig. 2, while the DM value for the extracellular coil is of the opposite direction (in the y axis projection, see Fig. 2 arrows *2* and *3*) and is equal to 554.45 D with opposite orientation as indicated by arrow *3*. By summing up both these DM values we get 614.24 D (see arrow *4* in Fig. 2). The DM value of the transmembrane helices is equal to 574.98 D as depicted by arrow *5* (Fig. 2) and is of the opposite direction (in the z axis projection). Retinal belongs to the photoactive centre of BR and its DM value is small giving 0.56 D as follows from the QM calculations. The QM calculations of the retinal together with Lys 216 (RETLYS) taken from the BR1 structure provide the value of 6.48 D for the DM with the orientation coinciding with direction of the DM of BR. It is worthwhile to mention that the DM corresponding to transmembrane helices as well as of the bound water molecules is of the opposite direction in comparison with the total DM determined by other constituents of the protein.

Similar calculations have been performed for BR-K, BR-L1, and BR-M1 structures. The BR-K structure corresponding to the K state is defined with 1.43 Å resolutions [30]. The monomer of BR-K also contains 2073 atoms including, however, various external constituents. Due to protonation of the Schiff base, it is also positively charged in the RETLYS fragment. The DM in this case is 248.87 D ($p_{BR} = -83.43$ D). After additional MM minimization the DM changes reaching 226.82 D with $p_{BR} = -57.86$ D. Next structure, BR-L1, evidently corresponding to the L1 state, is defined with 1.53 Å resolutions [31]. The monomer of BR-L1 consists of 1736 atoms (also skipping the hydrogen atoms) and the Schiff base remaining protonated. The calculated value of the DM amounts to 254.40 D and giving p_{BR} as much as -114.26 D. After MM minimization of the structure the DM slightly changes up to 239.47 D and p_{BR} turns to be equal to -91.61 D. The last structure under consideration, BR-M1, corresponding to the M1 state is defined with 1.43 Å resolutions [32]. The

monomer of BR-M1 consists of 2073 atoms (except for the hydrogen atoms) including various external constituents. In this case the Schiff base is not protonated anymore, while ASP85 is becoming protonated. The DM as calculated from this structure is 252.73 D, while p_{BR} is -99.11 D. After MM minimization of the structure the DM also changes up to 232.55 D and p_{BR} up to -41.95 D.

The same partition of the BR structure into the internal coil, the cytoplasmic and extracellular coils, as well as for the transmembrane helices has been invoked for the BR-L1 and BR-M1 structures. The DMs corresponding to the transmembrane helices in the BR-K and BR-M1 structures (not minimized) change by 34.47 and -33.24 D, respectively, in comparison with those values corresponding to the BR1 structure. The same substructures have similar values for BR-L1. The DM of the extracellular coil of the protein varies within 5.75 D for all BR structures. The DM of the cytoplastic coil of the protein varies in the range of 173.23 D when taken from different structures. However, qualitatively the directions of all DM are oriented similarly as shown in Fig. 2, with changes of the angles less than 30 deg.

Crystallographic data of BR under consideration, i. e. structures of BR1, BR-K, BR-L1, and BR-M1, provide the information with resolution from 1.4 to 1.62 Å. Additional minimization based on the MM calculations slightly modifies positions of atoms in these particular structures resulting in changes of the DM values up to 32 D for all structures, except for the BR-K case. Various DM values of K, L, and M states are presented in Fig. 3(a). The highest effect due to structural changes is obtained for the transmembrane helices as evidenced in Table 1. The DM for the BR-K structure before and after minimization procedure differs up to 50 D. However, it has a minor effect on the total DM due to the DM orientation.

The results of our MM calculations show that investigated structures have not changed essentially during minimization procedure. Various intermediates have similar relative dipole moment values before and after minimization (Fig. 3(a)). That leads us to conclusion that BR structures after minimization procedure belong to the same ground and intermediate structures as determined from crystallographic data.

It is noteworthy that the DM direction in K (BR-K), L (BR-L1), and M (BR-M1) states slightly varies. These variations are within 5 deg for most of the calculated dipole moments indicated by arrows, except the direction indicated by the 3rd arrow, where difference reaches up to 30 deg. However, these variations do not change the sign of the DM projection along the z axis (see Table 1).

4. Discussion

The QM/MM calculations are applied for the high-resolution X-ray structures of BR by considering various intermediate states (up to the M and N) by determining details of the sequential rearrangement of the protein [3, 29, 30, 32, 39–47]. Recently QM/MM calculation methods have been also invoked for estimations of the delocalization extent of the positive charge in the vicinity of Glu204 and Glu194 in BR [48, 49]. Instructive insight into the primary proton transfer rate has been also given by means of the same QM/MM approach [50, 51]. However, these calculations have not shown consistency with the observed pKa values as follows from the appropriate analysis [52–55]. Possible relationship between details of the 1C3W structure [29] has been analysed in terms of *ab initio* QM/MM calculations [56, 57]. Thus, our approach by estimating the DM of BR is well grounded.

As follows from the electro-acoustic measurements of dried films of the PMs, the projection of the DM of BR normal to the membrane surface is close to 40 D. The same value defined from QM/MM calculations for the BR1 structure is comparable to this value and of the same direction as defined from the electro-acoustic measurements. According to the analysis based on the partition of the BR structure, the DM is defined by the total volume of BR. The dominant input to the DM value corresponds to the cytoplasmic and extracellular coils, while the DM corresponding to the active centre including retinal gives a minor input. The contribution of the transmembrane helices results in the DM of the opposite direction in comparison with the dominating input of the cytoplasmic and extracellular coils and, thus, partly compensating the total value of the DM. Any deformation of the structure in the course of the photocycle can result in changes of the DM value.

The critical value of the bias voltage defined from the electrostriction measurements does not depend on the acidification level used for the film preparation as follows from Fig. 1(a). This result allows us to conclude that the DM value remains unchanged in the dried films independently of the acidity conditions (Eq. 5), however, becoming sensitive to the external conditions when soaked in solution [22]. This controversial observation supports our conclusion about the dominant input from the external coils of the protein by determining the DM value. Evidently, the charges present

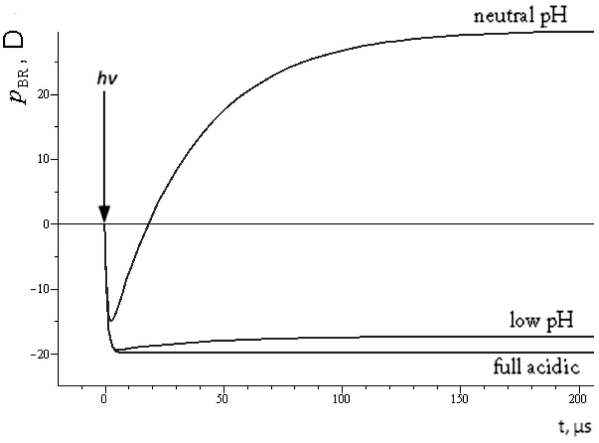

Fig. 4. Ensemble averaged time evolution of the projection of the mean value of the DM of BR on the z axis of the PM. In the case of neutral pH, all excited BR molecules reach the M intermediate state. Full acidic conditions correspond to the limiting case when the position for the proton in the first acceptor state is blocked by the external proton. Low acidic case corresponds to the mixture of BR in the film containing 90% with the totally blocked proton accepting state (the full acidic case) and the rest in the unblocked (neutral pH) state for the proton transfer.

in the solvent as well as the polarization of the solvent itself could have substantial influence on the DM value and even on its direction in this case. Such difference in sensitivity of the DM value depending on the surrounding of the PM (in the dried films versus solution) could be understood as follows. In the case of the dried film the dissociation ability of the acidic or alkali molecules might be hindered, in contrast to the situation in the solution. This is the reason why the surface charges of the PMs do not vary by changing the environmental conditions of the dried films.

Defined values of the DM in the intermediate states of the BR photocycle could be used to follow changes of this value and to attribute them to the driving force for the proton pumping. Indeed, by taking the DM values and their projections on the z axis in the BR1, L, and M states as schematically shown in Fig. 3(a), we can justify the model used by postulating the kinetic scheme for the proton transfer in the ensemble of BR molecules in the film [15]. The kinetics of the z axis projection of the total DM moment of the BR film then should follow the kinetics of the concentration of the relevant states in the photocycle. Thus, by choosing the evolution of these values as shown in Fig. 3(b) the temporal evolution of the projection value of the DM can be defined accordingly:

$$p_{\rm L} = p_{0\rm L}\,\frac{\tau_{\rm L}}{\tau_{\rm L}-\tau_0}\left(\mathrm{e}^{-t/\tau_{\rm L}}-\mathrm{e}^{-t/\tau_0}\right), \qquad (6)$$

$$p_{\rm M} = p_{0\rm M}\left[\frac{\tau_{\rm L}}{\tau_{\rm L}-\tau_0}\left(1-\mathrm{e}^{-t/\tau_{\rm L}}\right) - \frac{\tau_0}{\tau_{\rm L}-\tau_0}\left(1-\mathrm{e}^{-t/\tau_0}\right)\right], \quad \text{and} \qquad (7)$$

$$p_{\rm BR} = p_{\rm M} - p_{\rm L}\,, \qquad (8)$$

where $p_{\rm BR}$ represents the response of the film, $p_{0\rm L}$ and $p_{0\rm M}$ (see Fig. 3(b)) are the maximal values of the DM projection in the L and M states, while τ_0 and $\tau_{\rm L}$ are the lifetimes of the K and L intermediates, respectively. Substituting values $\tau_0 = 2$ μs and $\tau_{\rm L} = 50$ μs, we get the changes of this projection as shown in Fig. 4. Since the changes of the DM projection are proportional to the potential as defined from the experimental measurements (see Eq. (4)), the obtained kinetics totally reflects the kinetics defined from the experiments (see Fig. 10 from [15]). These results evidently support our previous conclusion that the changes of the electric field in the intermediates are related to the structural changes of the protein and, thus, demonstrate that the origin of the proton driving force should be attributed to the electrical-to-mechanical energy conversion taking place in the purple membrane.

In the acidic environment the $\tau_{\rm L}$ time constant corresponding to the transition from the L state to the M state should reflect the probability of the first proton acceptor D85 to be occupied by the external proton, accordingly [27]:

$$\tau_{\rm L} = \frac{1}{\nu_0\,\theta_{\rm SB}\,(1-\theta_{\rm D85})}\,\mathrm{e}^{W_{\rm L}/(kT)}\,, \qquad (9)$$

where ν_0 is the proton oscillation frequency in the initial state, $W_{\rm L}$ is the activation barrier energy of proton transfer from Schiff base to D85 acceptor.

The occupation factor of the Schiff base (SB) $\theta_{\rm SB} = 1$ and that of the acceptor D85 $\theta_{\rm D85} = 0$ correspond to the normal conditions when the proton is positioned in the initial state. At low pH of the environment the proton acceptor D85 is protonated, thus $\theta_{\rm D85} = 1$. Hence, from Eq. (9) we get that $\tau_{\rm L} = \infty$, and the resultant PERS of such BR molecules is

$$p_{\rm BR} = p_{0\rm L}\left(1-\mathrm{e}^{-t/\tau_0}\right), \qquad (10)$$

where $p_{\rm BR}$ represents the response of the film at very low pH (full acidic). Theoretical curves (see Fig. 4) were calculated using Eqs. (8) and (10) with the corresponding coefficients well correlating with the experimental data obtained for the oriented PM films under neutral and acidic conditions (see Fig. 1(b)). By comparing the calculated value of the time evolution of the

dipole moment (defined by Eqs. (6)–(8)) with the experimental observations presented in Fig. 1(b) we have to conclude that 90% of BR is blocked in the film under "low pH" conditions.

It should be noted that the value of the DM of BR in solution is variable depending on the pH value [26]. Such type of sensitivity supports our conclusion that the dominant value of the DM is defined by the external coils. Due to the variability of the surface charges on the pK values of the amino acids, changes of the DM value depending on the solvent conditions are expected (pK is dissociation constant value for one amino acid of BR molecule, in pH units).

The obtained value of the generated DM projection in the M intermediate reaches 30 D (see Fig. 3), similar to the experimental estimations. Taking into account the thickness of the purple membrane as $5{\cdot}10^{-9}$ m and assuming $\alpha = 1$, from Eq. (4) we could estimate the value of the electric potential generated accordingly, which is equal to 0.3 V. Remarkably, such electric potential is sufficient for ATP generation. The origin of all these changes of the DM value is predominantly defined by the protein deformation.

5. Conclusions

The PERS kinetics is usually attributed to the photoinduced proton pumping in the dried films of the PMs under normal external conditions and is suppressed under low pH conditions. From the analysis of the electroacoustic measurements of the dried films it is concluded that the projection of the p_{BR} value of BR along the direction normal to the membrane surface is of the order of 40 D and directed from the cytoplasmic side to the extracellular side of the PM. A similar value and the same orientation of p_{BR} are also deduced from the QM/MM calculations performed for the known crystallographic structures of the ground state of BR. These calculations demonstrate that the charged groups of the cytoplasmic and extracellular coils provide the dominant contribution by determining p_{BR}, while the contribution from the transmembrane helices and from the active centre is substantially smaller. Calculated p_{BR} values of BR in the L state are larger than those in the ground state and the BR structure in the M state. By taking these values of p_{BR} into account, the calculated PERS kinetics fits the experimental observations. As follows from these calculations, the electric potential generated in the M state of BR is 0.3 V. It is noteworthy that such electric potential is sufficient for ATP generation.

According to our QM/MM calculations the variability of the p_{BR} in the sequential states of BR is mainly defined by the conformational changes of the PM surfaces. These conformational changes are initiated by isomerization of retinal after its photoexcitation. The isomerization of retinal should induce stretching in the transmembrane helices, which in their turn initiate the conformational changes in the cytoplasmic and extracellular coils. The obtained strained conformation corresponds to the L intermediate state, which further on should relax, resulting in the M intermediate state formation. In the course of this relaxation the proton initially attached to the Schiff base starts moving due to the presence of the electrostatic potential corresponding to the L intermediate state seeking to screen it. Thus, the driving force for the proton transfer is a result of relaxation of the strained conformation of the protein in the L state.

It is found that the p_{BR} remains unchanged with acidification of the PM in the dried films, while the PERS kinetics substantially changes. Such sensitivity of the PERS to the pH changes can be understood by assuming the blockage possibility of the proton accepting state by the external protons. The reason why the surface charges of the PMs do not vary by changing the environmental conditions of the dried films as is deduced from the electro-acoustic measurements can be attributed to reduction of the dissociation ability of the acidic or alkali molecules under the dried film conditions.

Acknowledgement

This research was supported by the global grant of the Lithuanian Research Council according to the operational programme for the human resources development.

References

[1] D. Oesterhelt and W. Stoeckenius, Functions of a new photoreceptor membrane, Proc. Natl. Acad. Sci. USA **70**, 2853–2857 (1973).

[2] J.K. Lanyi, Proton translocation mechanism and energetics in the light-driven pump bacteriorhodopsin, Biochim. Biophys. Acta Bioenerg. **1183**, 241–261 (1993).

[3] J.K. Lanyi, Molecular mechanism of ion transport in bacteriorhodopsin: Insights from crystallographic, spectroscopic, kinetic, and mutational studies, J. Phys. Chem. B **104**, 11441–11448 (2000).

[4] R. Shinar, S. Druckmann, M. Ottolenghi, and R. Korenstein, Electric fields effect in bacteriorhodopsin, Biophys. J. **19**, 1–5 (1977).

[5] S. Saigo, The orientation of purple membranes in electric field, in: *Biological and Chemical Utilization of Solar Energy* (Gakkai Shuppan Center, Tokyo, 1978) pp. 127–131.

[6] L. Keszthelyi, Orientation of membrane fragments by electric field, Biochim. Biophys. Acta Biomembr. **598**, 429–436 (1980).

[7] S. Druckmann and M. Ottolenghi, Electric dichroism in the purple membrane of *Halobacterium halobium*, Biophys. J. **33**, 263–268 (1981).

[8] K. Tsuji and E. Neumann, Structural change in bacteriorhodopsin induced by electric impulses, Int. J. Biol. Macromol. **3**, 231–242 (1981).

[9] Y. Kimura, A. Ikegami, K. Ohno, S. Saigo, and Y. Takeuchi, Electric dichroism of purple membrane suspensions, Photochem. Photobiol. **33**, 435–439 (1981).

[10] G. Todorov, S. Sokerov, and S.P. Stoylov, Interfacial electric polarizability of purple membranes in solution, Biophys. J. **40**, 1–5 (1982).

[11] S.G. Taneva, G. Todorov, I.B. Petkanchin, and S.P. Stoylov, Electrooptic study of the deionized form of bacteriorhodopsin, Eur. Biophys. J. **14**, 415–421 (1987).

[12] Y. Kimura, M. Fujiwara, and A. Ikegami, Anisotropic electric properties of purple membrane and their change during the photoreaction cycle, Biophys. J. **45**, 615–625 (1984).

[13] J. Otomo, K. Ohno, Y. Takeuchi, and A. Ikegami, Surface charge movements of purple membrane during light-dark adaptation, Biophys. J. **50**, 205–211 (1986).

[14] S.G. Taneva and I.B. Petkanchin, Surface electric properties of biological systems, Trends Photochem. Photobiol. **6**, 113–139 (1999).

[15] P. Kietis, M. Vengris, and L. Valkunas, Electrical-to-mechanical coupling in purple membranes: membrane as electrostrictive medium, Biophys. J. **80**, 1631–1640 (2001).

[16] D. Porschke, Electrostatics and electrodynamics of bacteriorhodopsin, Biophys. J. **71**, 3381–3391 (1996).

[17] K. Barabas, A. Der, Z. Dancshazy, P. Ormos, L. Keszthelyi, and M. Marden, Electro-optical measurements on aqueous suspension of purple membrane from Halobacterium halobium, Biophys. J. **43**, 5–11 (1983).

[18] I.B. Petkanchin, S.G. Taneva, and G.S. Todorov, Influence of surface active substances on the electric surface properties of purple membrane fragments, Colloids Surf. **52**, 257–267 (1991).

[19] E. Papp, G. Fricsovszky, and G. Meszena, Electrodichroism of purple membrane: ionic strength dependence, Biophys. J. **49**, 1089–1100 (1986).

[20] R. Jonas, Y. Koutalos, and T.G. Ebrey, Purple membrane: surface charge density and the multiple effect of pH and cations, Photochem. Photobiol. **52**, 1163–1177 (1990).

[21] B. Ehrenberg and Y. Berezin, Surface potential on purple membranes and its sidedness studied by a resonance Raman dye probe, Biophys. J. **45**, 663–670 (1984).

[22] G. Varo, Dried oriented purple membrane samples, Acta Biol. Acad. Sci. Hung. **32**, 301–310 (1981).

[23] K.A. Fisher, K. Yanagimoto, and W. Stoeckenius, Oriented adsorption of purple membrane to cationic surfaces, J. Cell Biol. **77**, 611–620 (1978).

[24] I.G. Geza, L. Kelerman, A. Kulcsar, M. Lakatosand, and G. Varo, Photocycle of dried acid purple from of bacteriorhodopsin, Biophys. J. **81**, 3432–3441 (2001).

[25] L.D. Landau and E.M. Lifshitz, *Electrodynamics of Continuous Media* (Pergamon Press, Oxford U.K., 1960) pp. 36–91.

[26] G. Varo and L. Keszthelyi, Photoelectric signals from dried oriented purple membranes of Halobacterium halobium, Biophys. J. **43**, 47–51 (1983).

[27] P.B. Kietis, P. Saudargas, G. Váró, and L. Valkunas, External electric control of the proton pumping in bacteriorhodopsin, Eur. Biophys. J. **36**, 199–211 (2007).

[28] D.A. Case, T.A. Darden, T.E. Cheatham et al., *AMBER 9 Users' Manual* (University of California, San Francisco, 2006).

[29] H. Luecke, B. Schobert, H.T. Richter, J.P. Cartailler, and J.K. Lanyi, Structure of bacteriorhodopsin at 1.55 A resolution, J. Mol. Biol. **291**, 899–911 (1999).

[30] B. Schobert, J. Cupp-Vickery, V. Hornak, S. Smith, and J. Lanyi, Crystallographic structure of the K intermediate of bacteriorhodopsin: conservation of free energy after photoisomerization of the retinal, J. Mol. Biol. **321**, 715–726 (2002).

[31] J.K. Lanyi and B. Schobert, Structural changes in the L photointermediate of bacteriorhodopsin, J. Mol. Biol. **365**, 1379–1392 (2007).

[32] J. Lanyi and B. Schobert, Crystallographic structure of the retinal and the protein after deprotonation of the Schiff base: the switch in the bacteriorhodopsin photocycle, J. Mol. Biol. **321**, 727–737 (2002).

[33] N. Guex and M.C. Peitsch, SWISS-MODEL and the Swiss-PdbViewer: An environment for comparative protein modeling, Electrophoresis **18**, 2714–2723 (1997).

[34] M.J. Frisch, G.W. Trucks, H.B. Schlegel et al., *Gaussian 03, Revision C.02* (Gaussian, Inc., Wallingford CT, 2004).

[35] R.G. Parr and W. Yang, *Density Functional Theory of Atoms and Molecules* (Oxford University Press, Oxford, U.K., 1989).

[36] A.D. Becke, Density-functional thermochemistry. III. The role of exact exchange, J. Chem. Phys. **98**, 5648–5652 (1993).

[37] W. Humphrey, A. Dalke, and K. Schulten, VMD – visual molecular dynamics, J. Molec. Graphics **14**, 33–38 (1996).

[38] I. Ermolina, A. Strinkovski, A. Lewis, and Y. Felmon, Observation of liquid-crystal-like ferroelectric behavior in a biological membrane, J. Phys. Chem. B **105**, 2673–2676 (2001).

[39] B. Schobert, L.S. Brown, and J.K. Lanyi, Crystallographic structures of the M and N intermediates of bacteriorhodopsin: assembly of a hydrogen-bonded chain of water molecules between Asp96 and the retinal Schiff base, J. Mol. Biol. **330**, 553–570 (2003).

[40] J.K. Lanyi and B. Schobert, Mechanism of proton transport in bacteriorhodopsin from crystallographic structures of the K, L, M1, M2, and M2' intermediates of the photocycle, J. Mol. Biol. **328**, 439–450 (2003).

[41] K. Edman, P. Nollert, A. Royant, H. Belrhali, E. Pebay-Peyroula, J. Hajdu, R. Neutze, and E.M. Landau, High resolution X-ray structure of an early intermediate in the bacteriorhodopsin photocycle, Nature **401**, 822–826 (1999).

[42] K. Edman, A. Royant, G. Larsson, F. Jacobson, T. Taylor, S.D. Van Der, E.M. Landau, E. Pebay-Peyroula, and R. Neutze, Deformation of helix C in the low temperature L-intermediate of bacteriorhodopsin, J. Biol. Chem. **279**, 2147–2158 (2004).

[43] H.J. Sass, G. Buldt, R. Gessenich, D. Hehn, D. Neff, R. Schlesinger, J. Berendzen, and P. Ormos, Structural alterations for proton translocation in the M state of wild-type bacteriorhodopsin, Nature **406**, 649–653 (2000).

[44] T. Kouyama, T. Nishikawa, T. Tokuhisa, and H. Okumura, Crystal structure of the L intermediate of bacteriorhodopsin: evidence for vertical translocation of a water molecule during the proton pumping cycle, J. Mol. Biol. **335**, 531–546 (2004).

[45] K. Takeda, Y. Matsui, N. Kamiya, S. Adachi, H. Okumura, and T. Kouyama, Crystal structure of the M intermediate of bacteriorhodopsin: allosteric structural changes mediated by sliding movement of a transmembrane helix, J. Mol. Biol. **341**, 1023–1037 (2004).

[46] M.T. Facciotti, S. Rouhani, F.T. Burkard, F.M. Betancourt, K.H. Downing, R.B. Rose, G. McDermott, and R.M. Glaeser, Structure of an early intermediate in the M-state phase of the bacteriorhodopsin photocycle, Biophys. J. **81**, 3442–3455 (2001).

[47] Y. Matsui, K. Sakai, M. Murakami, Y. Shiro, S. Adachi, H. Okumura, and T. Kouyama, Specific damage induced by X-ray radiation and structural changes in the primary photoreaction of bacteriorhodopsin, J. Mol. Biol. **324**, 469–481 (2002).

[48] R. Rousseau, V. Kleinschmidt, U.W. Schmitt, and D. Marx, Modeling protonated water networks in bacteriorhodopsin, Phys. Chem. Chem. Phys. **6**, 1848–1859 (2004).

[49] G. Mathias and D. Marx, Structures and spectral signatures of protonated water networks in bacteriorhodopsin, Proc. Natl. Acad. Sci. USA **104**, 6980–6985 (2007).

[50] A.N. Bondar, S. Fischer, J.C. Smith, M. Elstner, and S. Suhai, Key role of electrostatic interactions in bacteriorhodopsin proton transfer, J. Am. Chem. Soc. **126**, 14668–14677 (2004).

[51] A.N. Bondar, M. Elstner, S. Suhai, J.C. Smith, and S. Fischer, Mechanism of primary proton transfer in bacteriorhodopsin, Structure **12**, 1281–1288 (2004).

[52] Y.F. Song, J.J. Mao, and M.R. Gunner, Calculation of proton transfers in bacteriorhodopsin bR and M intermediates, Biochemistry **42**, 9875–9888 (2003).

[53] A.M. Ferreira and D. Bashford, Model for proton transport coupled to protein conformational change: Application to proton pumping in the bacteriorhodopsin photocycle, J. Am. Chem. Soc. **128**, 16778–16790 (2006).

[54] V.Z. Spassov, H. Luecke, K. Gerwert, and D. Bashford, pKa calculations suggest storage of an excess proton in a hydrogen-bonded water network in bacteriorhodopsin, J. Mol. Biol. **312**, 203–219 (2001).

[55] R.V. Sampogna and B. Honig, Environmental-effects on the protonation states of active-site residues in bacteriorhodopsin, Biophys. J. **66**, 1341–1352 (1994).

[56] S. Hayashi and I. Ohmine, Proton transfer in bacteriorhodopsin: Structure, excitation, IR spectra, and potential energy surface analyses by an ab initio QM/MM method, J. Phys. Chem. B **104**, 10678–10691 (2000).

[57] S. Hayashi, E. Tajkhorshid, and K. Schulten, Structural changes during the formation of early intermediates in the bacteriorhodopsin photocycle, Biophys. J. **83**, 1281–1297 (2002).

BAKTERIORODOPSINO DIPOLINIO MOMENTO ĮVERTINIMAS

B.P. Kietis [a], M. Mačernis [b], J. Šulskus [b], L. Valkūnas [a,b]

[a] *Fizinių ir technologijos mokslų centro Fizikos institutas, Vilnius, Lietuva*
[b] *Vilniaus universiteto Fizikos fakultetas, Vilnius, Lietuva*

Santrauka

Bakteriorodopsino elektrinis dipolinis momentas įvertintas iš purpurinių membranų sausose plėvelėse elektroakustinių matavimų. Nustatyta dipolinio momento projekcijos į membranos paviršiaus normalę vertė lygi 40 D, kryptis – nuo citoplazminės į išorinę membranos pusę bei nepriklauso (arba labai mažai priklauso) nuo aplinkos pH. Norint atskleisti dipolinio momento susidarymo prigimtį, buvo atlikti žinomų bakteriorodopsino pagrindinės ir tarpinių struktūrų QM/MM skaičiavimai, iš kurių paaiškėjo, kad dipolinis momentas daugiausia priklauso nuo citoplazminės ir išorinės pusės membranos nebaltyminių dalių. Tarpmembraninės spiralės dipolinio turimo momento dalis yra mažesnė ir nukreipta priešingai. Apskaičiuotoji aktyvaus centro dipolinio momento vertė, lyginant su visos struktūros momento verte, yra maža. Gautos bakteriorodopsino dipolinio momento vertės K, L ir M būsenoms leidžia geriau suprasti protonovaros prigimtį. Pagrindinės ir tarpinių būsenų dipolinio momento vertės, apskaičiuotos QM/MM metodu, buvo panaudotos eksperimentiškai gautam sausų plėvelių fotoelektriniam atsakui paaiškinti.